

Accurate cosmology from gravitational-lens time delays

S. H. Suyu^{1,2}

¹Department of Physics, University of California, Santa Barbara, CA 93106, USA
email: suyu@physics.ucsb.edu

²Kavli Institute for Particle Astrophysics and Cosmology, Stanford University,
452 Lomita Mall, Stanford, CA 94035, USA

Abstract. The time delays between the multiple images of a strong gravitational-lens system, together with a model of the lens-mass distribution, provide a one-step determination of the time-delay distance, and thus a measure of cosmological parameters, particularly the Hubble constant, H_0 . I review the recent advances in measuring time-delay distances, and present the current status of cosmological constraints based on gravitational-lens time delays. In particular, I report the time-delay distance measurements of two gravitational lenses and their implication for cosmology from a recent study by Suyu *et al.*

Keywords. distance scale, gravitational lensing

1. Introduction

Many profound questions about the Universe remain unanswered, even in the present era of so-called precision cosmography. What is the nature of dark energy and dark matter? How many families of relativistic particles are there? What are the masses of the neutrinos? Is general relativity the correct theory of gravity? Did the Universe undergo an inflationary phase in its early stages?

From an empirical point of view, the way to address these questions is by increasing the accuracy and precision of cosmographic experiments. In particular, a measurement of the local value of the Hubble constant, H_0 , to 1% precision (i.e. random errors) and accuracy (i.e. systematic errors) would provide key new insights into the nature of dark energy and its evolution, the mass of neutrinos and the total number of families of relativistic particles, the validity of general relativity, and the curvature of the Universe as a test of inflationary models (e.g., Freedman & Madore 2010; Riess *et al.* 2011; Weinberg *et al.* 2012; Reid *et al.* 2010; Sekiguchi *et al.* 2010; Suyu *et al.* 2012a). It is essential to develop multiple independent methods as a way to control for known systematic uncertainties, uncover new ones, and ultimately discover discrepancies that may reveal new fundamental physics. For example, a proven inconsistency between inferences at high redshift from the analysis of the cosmic microwave background (CMB), with results at lower redshift from supernova surveys would challenge the standard description of the evolution of the Universe over this redshift interval, and possibly lead to revisions of either our theory of gravity or of our assumptions about the nature of dark energy and dark matter.

One attractive probe of cosmology is represented by gravitational-lens time delays, which provide a one-step distance measurement. The idea of doing cosmography with time-delay lenses has been known for decades (Refsdal 1964) and is simple. When a source is observed through a strong gravitational lens, multiple images form (e.g., Schneider *et al.* 2006). If the source is variable in time, these multiple images show the pattern of variability delayed relative to each other owing to the path difference between

the light rays and also the gravitational delay from the lens. By careful monitoring of the image light curves, the time delays between the images can be measured (see, e.g., Courbin 2003). The absolute time delays can be converted into an absolute distance, the so-called ‘time-delay distance,’ using an accurate mass model of the gravitational lens (e.g., Blandford & Narayan 1992; Jackson 2007; Treu 2010; and references therein). This distance is a combination of three angular-diameter distances, and so is primarily sensitive to the Hubble constant and depends weakly on the other cosmological parameters (Coe & Moustakas 2009; Linder 2011). Gravitational time delays are a one-step cosmological method to determine the Hubble constant that is completely independent of the local cosmic distance ladder (Freedman *et al.* 2001, 2012; Riess *et al.* 2011; Reid *et al.* 2012).

To control the systematic errors, a substantial amount of effort and resources needs to be invested in these cosmological probes. For gravitational time delays, this has required several observational and modeling breakthroughs. Long-duration and well-sampled light curves are essential for obtaining accurate time delays in the presence of microlensing. Modern light curves have much higher photometric precision, sampling, and duration (Fassnacht *et al.* 2002; Courbin *et al.* 2011) compared to the early pioneering light curves (e.g., Lehar *et al.* 1992). Deep and high-resolution images of extended features in the source, and stellar kinematics of the main deflector, provide thousands of data points to constrain the lens-mass model, thus breaking the degeneracy between the distance and the gravitational potential of the lens that affected previous models constrained only by the positions of the lensed quasars (e.g., Schechter *et al.* 1997). Finally, cosmological numerical simulations can now be used to characterize the distribution of mass along the line of sight (LOS; Hilbert *et al.* 2009), which was usually neglected in early studies. These advances make gravitational lens time delays a precise cosmological probe. Suyu *et al.* (2010) demonstrated that, with sufficient ancillary data, a single gravitational lens (B1608+656) can yield a time-delay distance measured to 5% precision. In combination with the *Wilkinson Microwave Anisotropy Probe* five-year results (*WMAP5*; Komatsu *et al.* 2009), the B1608+656 time-delay distance constrained H_0 to 7% and w to 18% precision, comparable to contemporary baryon acoustic oscillation experiments (Percival *et al.* 2007).

In this contribution, I summarize the results of a blind analysis of RXJ1131–1231 based on new and existing ancillary data on the lens system (Suyu *et al.* 2012b). The purpose of the blind analysis is to uncover unknown systematic errors and avoid unconscious experimenter bias for testing the accuracy of the method.

2. Gravitational-Lens Time Delays as a Cosmological Probe

This section briefly reviews the use of gravitational-lens time delays to study cosmology. More details on the subject can be found in, e.g., Schneider *et al.* (2006), Jackson (2007), Treu (2010), and Suyu *et al.* (2010).

In a gravitational-lens system, the excess time delay of an image at angular position $\theta = (\theta_1, \theta_2)$ with corresponding source position $\beta = (\beta_1, \beta_2)$, relative to the case of no lensing, is

$$t(\theta, \beta) = \frac{D_{\Delta t}}{c} \left[\frac{(\theta - \beta)^2}{2} - \psi(\theta) \right], \quad (2.1)$$

where $D_{\Delta t}$ is the so-called time-delay distance, c the speed of light, and $\psi(\theta)$ the lens potential. The first term in the square brackets corresponds to the geometric time delay due to the path difference, and the second term is the gravitational time delay owing

to the lens-mass distribution. The time-delay distance is a combination of the angular-diameter distance to the lens (or deflector; D_d) at redshift z_d , to the source (D_s), and between the lens and the source (D_{ds}):

$$D_{\Delta t} \equiv (1 + z_d) \frac{D_d D_s}{D_{ds}}. \quad (2.2)$$

For lens systems whose sources vary with time (such as active galactic nuclei; AGN), one can monitor the brightnesses of the lensed images as a function of time, and hence measure the time delay, Δt_{ij} , between the images at positions θ_i and θ_j :

$$\begin{aligned} \Delta t_{ij} &\equiv t(\theta_i, \beta) - t(\theta_j, \beta) \\ &= \frac{D_{\Delta t}}{c} \left[\frac{(\theta_i - \beta)^2}{2} - \psi(\theta_i) - \frac{(\theta_j - \beta)^2}{2} + \psi(\theta_j) \right]. \end{aligned} \quad (2.3)$$

One can model the mass distribution of the lens to determine the lens potential, $\psi(\theta)$, and the unlensed source position, β , by considering the image configuration and morphology. Lens systems with time delays can thus be used to measure $D_{\Delta t}$ based on Eq. (2.3), and constrain cosmological models through the distance–redshift test (e.g., Refsdal 1964, 1966; Fadely *et al.* 2010; Suyu *et al.* 2010). With dimensions of distance, $D_{\Delta t}$ is inversely proportional to H_0 , and as a combination of three angular-diameter distances, it depends weakly on the other cosmological parameters as well.

The radial slope of the lens-mass distribution has a direct influence on $D_{\Delta t}$: for a given time delay, a galaxy with a steep radial profile leads to a lower $D_{\Delta t}$ than a galaxy with a shallow profile (e.g., Witt *et al.* 2000; Wucknitz 2002; Kochanek 2002). Thus, it is necessary to determine the radial slope of the lens galaxy to measure $D_{\Delta t}$ accurately. Several authors have shown that spatially extended sources (such as the AGN host galaxy in time-delay lenses) can be used to measure the radial slope at the image positions, where it matters (e.g., Dye & Warren 2005; Dye *et al.* 2008; Suyu *et al.* 2010; Vegetti *et al.* 2010; Suyu 2012).

In addition to the mass distribution associated with the lens galaxy, LOS mass structures also affect the observed time delays. The external masses and voids cause additional focusing and defocusing of the light rays, respectively, and thus impact the time delays and $D_{\Delta t}$ inferences. The effect of the LOS structures is characterized by a single parameter, the external convergence κ_{ext} , with positive values associated with overdense LOSs and negative values with underdense LOSs (e.g., Keeton 2003; Suyu *et al.* 2010).

Given the measured time delays between the multiple images of a lens system, a mass model that does not account for κ_{ext} leads to an under/overprediction of $D_{\Delta t}$ for an over/underdense LOS. In particular, the true $D_{\Delta t}$ is related to the modeled parameter by

$$D_{\Delta t} = \frac{D_{\Delta t}^{\text{model}}}{1 - \kappa_{\text{ext}}}. \quad (2.4)$$

There are two practical approaches to overcoming this degeneracy: (i) using the stellar kinematics of the lens galaxy (e.g., Treu & Koopmans 2002, 2004; Koopmans & Treu 2003; Barnabè *et al.* 2009, 2011; Auger *et al.* 2010; Suyu *et al.* 2010; Sonnenfeld *et al.* 2012) to determine an independent estimate of the lens mass, and (ii) studying the environment of the lens system (e.g., Keeton & Zabludoff 2004; Fassnacht *et al.* 2006, 2011; Momcheva *et al.* 2006; Suyu *et al.* 2010; Wong *et al.* 2011) to estimate κ_{ext} directly. In the analysis of RXJ1131–1231 (Suyu *et al.* 2012b), we combined both approaches to infer κ_{ext} .

3. Cosmological Constraints from Time-Delay Distances

To measure the time-delay distance to RXJ1131–1231 with all known sources of systematic uncertainty taken into account, the following ancillary data have been assembled (Suyu *et al.* 2012b):

- Observed time delays with $< 2\%$ uncertainty based on dedicated and long-duration monitoring by COSMOGRAIL (COSmological MONitoring of GRAvItational Lenses; e.g., Vuissoz *et al.* 2008; Courbin *et al.* 2011) and Kochanek *et al.* collaborations (e.g., Kochanek *et al.* 2006), and newly developed curve-shifting techniques (Tewes *et al.* 2012a,b).
- Deep and high-resolution imaging of the lensed arcs based on *Hubble Space Telescope* (*HST*) observations. Combined with our flexible modeling techniques that use the thousands of surface brightness pixels of the lensed source as data, the archival *HST* images allow constraints on the potential difference between the lensed images—in Eq. (2.3)—at the few-percent level.
- Stellar velocity dispersion of the lens galaxy from spectra taken at the *Keck* Observatory and information about the lens environment. The stellar velocity dispersion of the lens galaxy provides constraints on both the lens-mass distribution and the external convergence. Furthermore, observations of galaxy counts in the fields of lenses (Fassnacht *et al.* 2011), together with ray tracing through numerical simulations of large-scale structure (e.g., Hilbert *et al.* 2007), constrain directly and statistically κ_{ext} at the $\sim 5\%$ level.

With these data sets, we measured $D_{\Delta t}$ to RXJ1131–1231 with 6% precision, including all sources of known uncertainty (Suyu *et al.* 2012b). The analysis was blinded to avoid experimenter bias, allowing tests for the presence of residual systematics in the analysis technique. As described by Conley *et al.* (2006), the blinding was not meant to hide all information from the experimenter; rather, only the parameters that concerned the cosmological inference were blinded.

There were two analysis phases, as detailed in Suyu *et al.* (2012b). During the initial ‘blind’ phase, we sampled the posterior probability distribution function (PDF) of the model parameters, taking care to only make parameter-space plots using one plotting code. This piece of software added offsets to the cosmological parameters before displaying the PDFs, such that we always viewed the marginalized distributions with centroids at exactly zero. We could therefore still see, and measure, the *precision* of the blinded parameters, and visualize the correlations between these parameters, but without being able to see if we had obtained ‘the right answer.’ Both the parameter uncertainties and degeneracies served as useful checks during this blind phase: the plotting routine could overlay the constraints from different models to investigate sources of statistical and systematic uncertainties. During the blind phase we performed a number of tests on the modeling to quantify the sources of uncertainties and check the robustness of the results. After all coauthors agreed that the blind analysis was complete, and that results would be published without modification once unblinded, a script was run to update automatically the plots and tables containing cosmological constraints no longer offset to zero.

Fig. 1 shows the blinded cosmological constraints from RXJ1131–1231 in the left-hand panel and the unblinded results in the right-hand panel. The shaded contours are the results based on the time-delay distance measurement to RXJ1131–1231 and the *WMAP* seven-year results (Komatsu *et al.* 2011) in a flat w CDM cosmology. The time-delay distance is mostly sensitive to H_0 , and the constraint on H_0 breaks the parameter degeneracies in the *WMAP7* data set. We obtain the following joint parameter constraints for RXJ1131–1231 in combination with *WMAP7*: $H_0 = 80.0^{+5.8}_{-5.7}$ km s $^{-1}$ Mpc $^{-1}$, $\Omega_{\text{de}} = 0.79 \pm 0.03$, and $w = -1.25^{+0.17}_{-0.21}$.

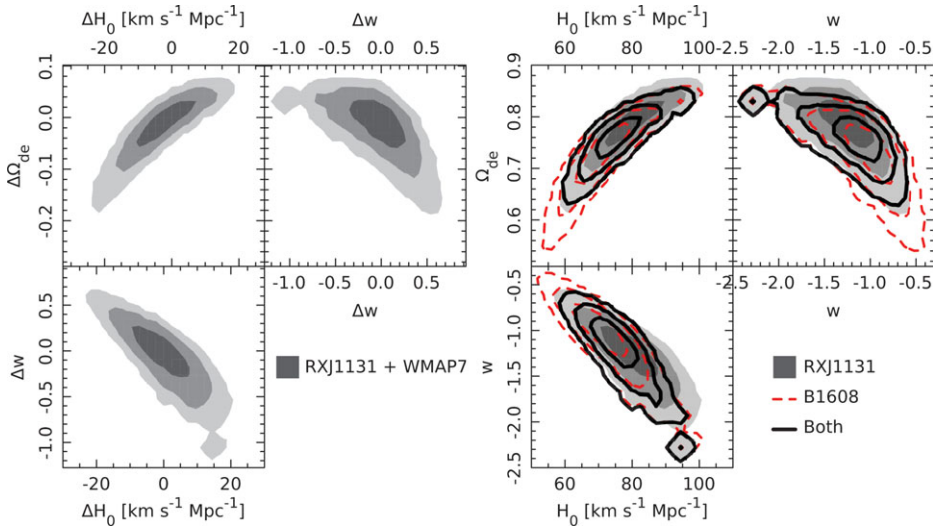


Figure 1. Blinded (left) and unblinded (right) posterior PDFs for H_0 , Ω_{de} , and w in flat w CDM cosmological models in combination with *WMAP* seven-year results (Komatsu *et al.* 2011). The shaded, dashed, and solid contours correspond to constraints from RXJ1131–1231, B1608+656, and both lenses, respectively. Contours/shades mark the 68.3%, 95.4%, and 99.7% credible regions. (*This figure has been adapted from Suyu et al. 2012b.*)

How do the results based on RXJ1131–1231 compare with those from B1608+656? In Fig. 1, the cosmological constraints from B1608+656 are shown as dashed contours, which partly overlap with those from RXJ1131–1231. To investigate the consistency between both lenses, we need to consider their likelihood functions in the multi-dimensional cosmological parameter space: inconsistency is defined by insufficient overlap between the two likelihoods. We follow Marshall *et al.* (2006), and compute the Bayes factor, F , in favor of a single set of cosmological parameters and a simultaneous fit:

$$F = \frac{\langle L^R L^B \rangle}{\langle L^R \rangle \langle L^B \rangle}, \tag{3.1}$$

where L^R and L^B are the likelihoods of the RXJ1131–1231 and B1608+656 data respectively, computed at each prior sample point. As detailed in Suyu *et al.* (2012b), the Bayes factor takes the value 3.8, indicating that the two lenses favor a single set of cosmological parameters. In other words, the results from RXJ1131–1231 and B1608+656 are consistent with each other.

Since RXJ1131–1231 and B1608+656 are consistent with each other, they can be combined for cosmological inferences. Fig. 1 shows the cosmological constraints from the two lenses in combination with *WMAP7* as solid contours. By combining the two lenses, we tighten the constraints on H_0 and Ω_{de} , whereas the precision of w does not improve appreciably. With its low lens redshift of 0.295, RXJ1131–1231 provides very little information about w in addition to that obtained from B1608+656. The marginalized constraints from the two lenses are $H_0 = 75.2^{+4.4}_{-4.2}$ km s⁻¹ Mpc⁻¹, $\Omega_{de} = 0.76^{+0.02}_{-0.03}$, and $w = -1.14^{+0.17}_{-0.20}$ in a flat w CDM Universe.

How do the time-delay distances from the two lenses compare to the distance measures based on other probes? In Fig. 2 we show a comparison of the cosmological constraints from the two lenses, baryon acoustic oscillations (BAO; e.g., Percival *et al.* 2010; Blake *et al.* 2011; Mehta *et al.* 2012), and supernovae (SNe; e.g., Hicken *et al.* 2009; Suzuki *et al.*

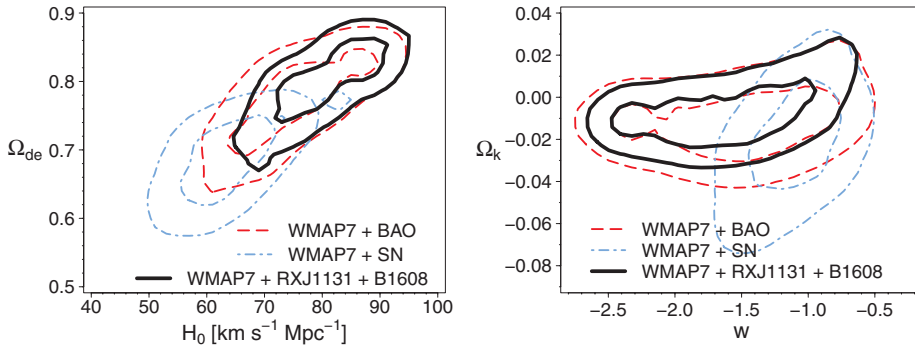


Figure 2. Comparison of cosmological probes. Posterior PDF of H_0 , Ω_{de} , w , and Ω_k for BAO (red dashed; Percival *et al.* 2010), SNe (blue dot-dashed; Hicken *et al.* 2009), time-delay lenses (black solid; Suyu *et al.* 2012b) when each is combined with *WMAP7* (Komatsu *et al.* 2011) in an open w CDM cosmology. Contours mark the 68% and 95% credible regions. Time-delay lenses are highly complementary to other probes, particularly CMB and SNe. (*This figure has been adapted from Suyu et al. 2012b.*)

2012), when each is combined with *WMAP7* in the open (non-flat) w CDM cosmology. The figure is only qualitative since the samples for the *WMAP7* chain in the open w CDM cosmology are sparse and the contours have been smoothed. Nonetheless, the sizes of the contours are comparable, suggesting that even a small sample of time-delay lenses is a powerful probe of cosmology. Both the lenses and BAO are strong in constraining the curvature of the Universe, while SNe provide more information on the dark energy's equation of state. Lenses are thus highly complementary to other cosmographic probes, particularly the CMB and SNe (see also, e.g., Linder 2011; Das & Linder 2012). Each probe is consistent with a flat Λ CDM cosmology: $\Omega_k = 0$ and $w = -1$ are within the 95% credible regions.

4. Summary

Gravitational-lens time delays provide a one-step measurement of a cosmological distance, the time-delay distance to the lens, which is completely independent of the local distance ladder. I have described recent advances in measuring time-delay distances and summarized the cosmological constraints from two time-delay lenses, RXJ1131–1231 and B1608+656, in Suyu *et al.* (2012b). In particular,

(a) The blind analysis of the time-delay lens RXJ1131–1231 yielded a robust time-delay distance measurement of 6% precision that took into account all sources of known statistical and systematic uncertainty. A fitting formula to describe the PDF of the time-delay distance is provided in Suyu *et al.* (2012b). It can be used to combine with any other independent cosmological probe.

(b) The time-delay distance of RXJ1131–1231 is mostly sensitive to H_0 . The constraint on H_0 helps break parameter degeneracies in the CMB data. In combination with *WMAP7*, Suyu *et al.* (2012b) measured $H_0 = 80.0^{+5.8}_{-5.7}$ km s⁻¹ Mpc⁻¹, $\Omega_{de} = 0.79 \pm 0.03$, and $w = -1.25^{+0.17}_{-0.21}$ in a flat w CDM cosmology. These are statistically consistent with the results from the gravitational lens B1608+656.

(c) By combining RXJ1131–1231, B1608+656, and *WMAP7*, Suyu *et al.* (2012b) derived the following constraints in a flat w CDM Universe: $H_0 = 75.2^{+4.4}_{-4.2}$ km s⁻¹ Mpc⁻¹, $\Omega_{de} = 0.76^{+0.02}_{-0.03}$, and $w = -1.14^{+0.17}_{-0.20}$.

(d) A comparison of the lenses and other cosmological probes, when each is combined with *WMAP7*, shows that the constraints from the lenses are comparable in precision to various state-of-the-art probes. Lenses are particularly powerful in measuring the spatial curvature of the Universe, and are complementary to other cosmological probes.

Dedicated monitoring of lens systems (particularly by the COSMOGRAIL and Kochanek *et al.* [2006] collaborations) has led to a significant increase in the number of lenses with accurate and precise time delays. Deep *HST* imaging for three of these lenses will be obtained in Cycle 20, to allow accurate lens-mass modeling that turns the delays into distances. Current and upcoming telescopes and surveys including the Panoramic Survey Telescope & Rapid Response System, the Hyper-Suprime Camera on the Subaru Telescope, and the Dark Energy Survey expect to detect hundreds of AGN lenses with dozens of delays measured (Oguri & Marshall 2010). Furthermore, the Large Synoptic Survey Telescope will discover thousands of time-delay lenses, painting a bright future for cosmography with gravitational-lens time delays.

References

- Auger, M. W., Treu, T., Bolton, A. S., *et al.* 2010, *ApJ*, 724, 511
- Barnabè, M., Czoske, O., Koopmans, L. V. E., Treu, T., & Bolton, A. S. 2011, *MNRAS*, 415, 2215
- Barnabè, M., Czoske, O., Koopmans, L. V. E., *et al.* 2009, *MNRAS*, 399, 21
- Blake, C., Davis, T., Poole, G. B., *et al.* 2011, *MNRAS*, 415, 2892
- Blandford, R. D. & Narayan, R. 1992, *ARA&A*, 30, 311
- Coe, D. & Moustakas, L. A. 2009, *ApJ*, 706, 45
- Conley, A., Goldhaber, G., Wang, L., *et al.* 2006, *ApJ*, 644, 1
- Courbin, F. 2003, in: *Gravitational Lensing: a unique tool for cosmology* (astro-ph/0304497)
- Courbin, F., Chantry, V., Revaz, Y., *et al.* 2011, *A&A*, 536, A53
- Das, S. & Linder, E. V. 2012, *Phys. Rev. D*, 86, 063520
- Dye, S., Evans, N. W., Belokurov, V., Warren, S. J., & Hewett, P. 2008, *MNRAS*, 388, 384
- Dye, S. & Warren, S. J. 2005, *ApJ*, 623, 31
- Fadely, R., Keeton, C. R., Nakajima, R., & Bernstein, G. M. 2010, *ApJ*, 711, 246
- Fassnacht, C. D., Gal, R. R., Lubin, L. M., *et al.* 2006, *ApJ*, 642, 30
- Fassnacht, C. D., Koopmans, L. V. E., & Wong, K. C. 2011, *MNRAS*, 410, 2167
- Fassnacht, C. D., Xanthopoulos, E., Koopmans, L. V. E., & Rusin, D. 2002, *ApJ*, 581, 823
- Freedman, W. L. & Madore, B. F. 2010, *ARA&A*, 48, 673
- Freedman, W. L., Madore, B. F., Scowcroft, V., *et al.* 2012, *ApJ*, 758, 24
- Freedman, W. L., Madore, B. F., Gibson, B. K., *et al.* 2001, *ApJ*, 553, 47
- Hicken, M., Wood-Vasey, W. M., Blondin, S., *et al.* 2009, *ApJ*, 700, 1097
- Hilbert, S., Hartlap, J., White, S. D. M., & Schneider, P. 2009, *A&A*, 499, 31
- Hilbert, S., White, S. D. M., Hartlap, J., & Schneider, P. 2007, *MNRAS*, 382, 121
- Jackson, N. 2007, *Liv. Rev. Rel.*, 10, 4
- Keeton, C. R. 2003, *ApJ*, 584, 664
- Keeton, C. R. & Zabludoff, A. I. 2004, *ApJ*, 612, 660
- Kochanek, C. S. 2002, *ApJ*, 578, 25
- Kochanek, C. S., Morgan, N. D., Falco, E. E., *et al.* 2006, *ApJ*, 640, 47
- Komatsu, E., Dunkley, J., Nolta, M. R., *et al.* 2009, *ApJS*, 180, 330
- Komatsu, E., Smith, K. M., Dunkley, J., *et al.* 2011, *ApJS*, 192, 18
- Koopmans, L. V. E. & Treu, T. 2003, *ApJ*, 583, 606
- Lehar, J., Hewitt, J. N., Burke, B. F., & Roberts, D. H. 1992, *ApJ*, 384, 453
- Linder, E. V. 2011, *Phys. Rev. D*, 84, 123529
- Marshall, P., Rajguru, N., & Slosar, A. 2006, *Phys. Rev. D*, 73, 067302
- Mehta, K. T., Cuesta, A. J., Xu, X., Eisenstein, D. J., & Padmanabhan, N. 2012, *MNRAS*, submitted (arXiv:1202.0092)

- Momcheva, I., Williams, K., Keeton, C., & Zabludoff, A. 2006, *ApJ*, 641, 169
- Oguri, M. & Marshall, P. J. 2010, *MNRAS*, 405, 2579
- Percival, W. J., Cole, S., Eisenstein, D. J., *et al.* 2007, *MNRAS*, 381, 1053
- Percival, W. J., Reid, B. A., Eisenstein, D. J., *et al.* 2010, *MNRAS*, 401, 2148
- Refsdal, S. 1964, *MNRAS*, 128, 307
- Refsdal, S. 1966, *MNRAS*, 132, 101
- Reid, B. A., Percival, W. J., Eisenstein, D. J., *et al.* 2010, *MNRAS*, 404, 60
- Reid, M. J., Braatz, J. A., Condon, J. J., *et al.* 2012, *ApJ*, submitted (arXiv:1207.7292)
- Riess, A. G., Macri, L., Casertano, S., *et al.* 2011, *ApJ*, 730, 119
- Schechter, P. L., Baily, C. D., Barr, R., *et al.* 1997, *ApJ*, 475, L85
- Schneider, P., Kochanek, C. S., & Wambsganss, J. 2006, *Gravitational Lensing: Strong, Weak and Micro* (Springer)
- Sekiguchi, T., Ichikawa, K., Takahashi, T., & Greenhill, L. 2010, *JCAP*, 3, 15
- Sonnenfeld, A., Treu, T., Gavazzi, R., *et al.* 2012, *ApJ*, 752, 163
- Suyu, S. H. 2012, *MNRAS*, 426, 868
- Suyu, S. H., Marshall, P. J., Auger, M. W., *et al.* 2010, *ApJ*, 711, 201
- Suyu, S. H., Treu, T., Blandford, R. D., *et al.* 2012a, arXiv:1202.4459
- Suyu, S. H., Auger, M. W., Hilbert, S., *et al.* 2012b, *ApJ*, submitted (arXiv:1208.6010)
- Suzuki, N., Rubin, D., Lidman, C., *et al.* 2012, *ApJ*, 746, 85
- Tewes, M., Courbin, F., & Meylan, G. 2012a, *A&A*, submitted (arXiv:1208.5598)
- Tewes, M., Courbin, F., Meylan, G., *et al.* 2012b, *A&A*, submitted (arXiv:1208.6009)
- Treu, T. 2010, *ARA&A*, 48, 87
- Treu, T. & Koopmans, L. V. E. 2002, *MNRAS*, 337, L6
- Treu, T. & Koopmans, L. V. E. 2004, *ApJ*, 611, 739
- Vegetti, S., Koopmans, L. V. E., Bolton, A., Treu, T., & Gavazzi, R. 2010, *MNRAS*, 408, 1969
- Vuissoz, C., Courbin, F., Sluse, D., *et al.* 2008, *A&A*, 488, 481
- Weinberg, D. H., Mortonson, M. J., Eisenstein, D. J., *et al.* 2012, arXiv:1201.2434
- Witt, H. J., Mao, S., & Keeton, C. R. 2000, *ApJ*, 544, 98
- Wong, K. C., Keeton, C. R., Williams, K. A., Momcheva, I. G., & Zabludoff, A. I. 2011, *ApJ*, 726, 84
- Wucknitz, O. 2002, *MNRAS*, 332, 951